TITLE: Test Cases for the Benchmark Active Controls Model: Spoiler and Control Surface Oscillations and Flutter

8E. TEST CASES FOR THE BENCHMARK ACTIVE CONTROLS MODEL: SPOILER AND CONTROL SURFACE OSCILLATIONS AND FLUTTER

Submitted by

Robert M. Bennett
Senior Aerospace Engineer
r.m.bennett@larc.nasa.gov

Robert C. Scott
Aerospace Engineer
r.c.scott @larc.nasa.gov

Carol D. Wieseman
Aerospace Engineer
c.d.wieseman @larc.nasa.gov

Aeroelasticity Branch, Structures and Materials
Mail Stop 340
NASA Langley Research Center
Hampton, VA 23681-2199 USA

INTRODUCTION

As a portion of the Benchmark Models Program at NASA Langley (Ref 1-2), a simple generic model was developed for active controls research and was called BACT for Benchmark Active Controls Technology model. This model was based on the previously-tested Benchmark Models rectangular wing with the NACA 0012 airfoil section that was mounted on the Pitch and Plunge Apparatus (PAPA) for flutter testing (Ref 1, 3-5). The BACT model had an upper surface spoiler, a lower surface spoiler, and a trailing edge control surface for use in flutter suppression and dynamic response excitation. Previous experience with flutter suppression (Ref 6-7) indicated a need for measured control surface aerodynamics for accurate control law design. Three different types of flutter instability boundaries had also been determined for the NACA 0012/PAPA model, a classical flutter boundary, a transonic stall flutter boundary at angle of attack, and a plunge instability near M = 0.9 (Ref 1, 3-5). Therefore an extensive set of steady and control surface oscillation data was generated spanning the range of the three types of instabilities (Ref 8). This information was subsequently used to design control laws to suppress each flutter instability.

There have been three tests of the BACT model. The objective of the first test, TDT Test 485, was to generate a data set of steady and unsteady control surface effectiveness data, and to determine the open loop dynamic characteristics of the control systems including the actuators. Unsteady pressures, loads, and transfer functions were measured. The other two tests, TDT Test 502 and TDT Test 518, were primarily oriented towards active controls research, but some data supplementary to the first test were obtained. Dynamic response of the flexible system to control surface excitation and open loop flutter characteristics were determined during Test 502. Loads were not measured during the last two tests. During these tests, a database of over 3000 data sets was obtained. A reasonably extensive subset of the data sets from the first two tests have been chosen for Test Cases for computational comparisons concentrating on static conditions and cases with harmonically oscillating control surfaces. Several flutter Test Cases from both tests have also been included.

Some aerodynamic comparisons with the BACT data have been made using computational fluid dynamics codes at the Navier-Stokes level in Ref 9-11 (and in the accompanying chapter 8C). Some mechanical and active control studies have been presented in Ref 12-17.

In this report several Test Cases are selected to illustrate trends for a variety of different conditions with emphasis on transonic flow effects. Cases for static angles of attack, static trailing-edge and upper-surface spoiler deflections are included for a range of conditions near those for the oscillation cases. Cases for trailing-edge control and upper-surface spoiler oscillations for a range of Mach numbers, angle of attack, and static control deflections are included. Cases for all three types of flutter instability are selected. In addition some cases are included for dynamic response measurements during forced oscillations of the controls on the flexible mount. An overview of the model and tests is given, and the standard formulary for these data is listed. Some sample data and sample results of calculations are presented. Only the static pressures and the first harmonic real and imaginary parts of the pressures are included in the data for the Test Cases, but digitized time histories have been archived. The data for the Test Cases are also available as separate electronic files.

LIST OF SYMBOLS AND DEFINITIONS

c	wing chord, ft (m)
C_p	pressure coefficient, $(p - p_\infty) / q_\infty$ steady; $(p - p_{mean}) / q_\infty$ unsteady
f	frequency, Hz
k	reduced frequency, $\omega c/(2V_\infty)$
M	Mach number
MILEA	model inboard leading edge accelerometer
MITEA	model inboard trailing edge accelerometer
MOLEA	model outboard leading edge accelerometer
MOTEA	model outboard trailing edge accelerometer
p	pressure, psf (kPa)
p_∞	freestream static pressure, psf (kPa)

q_∞	dynamic pressure, psf (kPa)
R_N	Reynolds number based on average chord
T_o	total or stagnation temperature, °R (°C)
V_∞	freestream velocity, ft/sec (m/sec)
x/c	streamwise fraction of local chord
y	spanwise coordinate normal to freestream
α_o	mean angle of attack, degrees
δ_{te}	trailing edge control surface deflection, degrees or radians, Fig 1
δ_{us}	upper spoiler deflection, degrees or radians, Fig 1
η	fraction of span, y/s
γ	ratio of specific heats for test gas
ω	frequency, radians/second
	subscript 0 = steady value

MODEL AND TESTS

The BACT model was tested in the NASA Langley Transonic Dynamics Tunnel (TDT). The tunnel has a slotted test section 16-feet (4.064 m) square with cropped corners. At the time of these tests, it could be operated with air or a heavy gas, R-12, as a test medium at pressures from very low to near atmospheric values. Currently the TDT can be operated with air or R-134a as a test medium. An early description of this facility is given in Ref 18 and more recent descriptions of the facility are given in Ref 19 and 20. The early data system is described in Ref 21 and the recent data system given in Ref 22 and 23, but the data system used in the BACT tests was a version between these systems. Based on cone transition results (Ref 24-25), the turbulence level for this tunnel is in the average large transonic tunnel category. Some low speed turbulence measurements in air have also been presented in Ref 26.

An overall view of the BACT model is shown in Fig 1. It is a rectangular planform wing with a span of 32 inches (813 mm) plus a tip of revolution and a chord of 16 inches (406 mm). It has a trailing edge control surface of 25 per cent chord, hinged at 75 per cent chord, extending between 45 percent and 75 percent span. Upper and lower surface spoilers of 15 per cent chord length were located directly ahead of the trailing edge control surface, were of the same span, and were hinged at 60 per cent chord (Fig 1). The outward surface of the spoilers was flat, and a relatively thin trailing edges extended to near the round leading edge radius of the trailing edge control surface. When both spoilers were deployed, the cavity underneath was open permitting flow between upper and lower surfaces. The cavity contained plumbing for the actuators, wiring, and the shape is undocumented. The wing was machined from aluminum and was very smooth (the screws for the hatch covers shown in Fig 1 were filled in for the tests) and was tested with a transition strip at 5 per cent chord. The control surfaces were of composite construction and were driven with miniature hydraulic actuators located within the wing.

The BACT model is shown installed in the TDT in Fig 2. It was mounted on a large splitter plate set out approximately 40 inches (1.02 m) from tunnel sidewall. The model had an end plate fixed to its root that moved with the model within a recessed or undercut section of the splitter plate. A large fairing behind the splitter plate isolated the equipment between the splitter plate and the tunnel sidewall from the airstream. Some recent tests (Ref 27) of the splitter plate arrangement without a wing have shown some nonuniformity of the flow resulting from the flow around the splitter plate leading edge for Mach numbers above M = 0.80 and the data may be somewhat affected.

The BACT model was tested with two different mounting systems shown in Fig 3. For the first test, TDT Test 485, a circular strut extended from the turntable to the balance that was attached to the wing for force measurements (Fig 3a). The model could be pitched statically with the turntable, and the controls were powered for static and dynamic measurements. Most of the Test Cases for control surface oscillation were determined from this setup.

The model was also tested using the Pitch and Plunge Apparatus (PAPA, Ref 28-29) as illustrated in Fig 3b. The PAPA system permits rigid body pitch and plunge motion of the wing and flutter of the system by using four circular rods for flexibility. This system has sufficient strength to permit flutter testing at moderate angles of attack including some stall flutter cases. The rods are arranged such that the elastic axis is at the midchord and the model is balanced to place the total center of gravity on the midchord. The system thus gives primarily pitch and plunge uncoupled modes about the midchord of the model. The summary of the modal parameters is given in Table 1. The generalized masses given here are the effective mass and pitch inertia calculated from the frequency and stiffness values. Higher modes of this system have been explored with a different model and given in Ref 30. Some amplitude effects on frequency and damping were presented in Ref 30 also, but may not apply to BACT as a result of the addition of hydraulic lines spanning the PAPA system. Detailed wind-off free decay records have been archived. A remotely operable restraining or snubber system was installed and was used to suppress flutter when it grew near the amplitude limits and many flutter points were obtained. Some additional mass parameters relating to the control surfaces are available in Ref 12-14.

Both the model and the plate that constrains the model end of the PAPA system are large in mass. The resulting mass ratio at flutter is thus very large and consequently the reduced frequency at flutter is very low. The flutter crossings are relatively mild and unpublished calculations have indicated some sensitivity to torsional aerodynamic damping.

The model was instrumented for unsteady pressures at two chords and for dynamic motions. The list of transducers is given in Table 2 and shown in Fig 4. There were 58 unsteady pressure transducers located along the chord at 60 per cent span that is at the midspan of the control surfaces. There were 5 transducers on each spoiler and 7 on each of the upper and lower surfaces of the trailing edge control surface. This relatively dense spacing of the transducers was selected to define the pressures near the control surface hinge lines. In addition there were 17 unsteady pressure transducers located at 40 percent span over the aft portion of the chord that were placed to examine the carry-over loading near the side edge of the control surfaces. Space limitations prevented further pressure instrumentation at other chords. It might be noted that some flow visualization work on these low aspect ratio planforms indicated that wing surface separation tended to occur in an inboard aft cell. The row of pressure transducers at 60 per cent chord was in the outer portion of this cell.

Dynamic data from all channels were acquired simultaneously at a rate of 500 samples/second and stored in digital form on disk. For the static data, at least 10 seconds of data was acquired for averaging and for the oscillating control cases, 8-10 seconds of data was acquired and analyzed. For the flutter cases, data was selected for nearly constant amplitude, and ran from 3 to 30 seconds. The number of samples used is included in the data files for the dynamic cases. Each recorded data set was assigned an index called a Point No. which is given in the Tables. Although it was intended to use 200 Hz low pass filters in the data stream prior to digitizing the data to avoid aliasing, the filters were later thought to be set at 1000 Hz as a result of a data system problem. The data are thus considered aliased with a foldover frequency of 250 Hz. For the flutter data, which was in the 4 to 10 Hz range, in order for the 1st harmonic to be contaminated, there would have to be significant signals at 490-510 Hz or at 990-996 Hz. It is not considered likely that there are significant disturbances in these frequency ranges.

Detailed geometry measurements were performed for this wing along several sections as illustrated in Fig 5. The measured ordinates are not included in this report, but they are available as an electronic file on the CD.

TEST CASES

An extensive set of Test Cases is selected with emphasis on transonic flow effects. The Test Case Number begins with 8E for the chapter identifier. There are several configurations and variables such that a few cases per configuration results in a fairly large number, but one would normally not be concerned with all configurations. The aerodynamic Test Cases selected generally include four Mach numbers, M = 0.65, which is subsonic at low angles of attack, M = 0.77, which is transonic and near the bottom of the flutter "bucket", M = 0.82, which is strongly transonic, and M = 0.90 which is significantly beyond normal applications for this airfoil. Control surface deflection cases are generally selected for angles of attack of zero and four degrees. It might be noted that the transition strip (at five per cent chord) has an influence on the first transducer downstream of the strip. The effect varies with angle of attack and other test conditions.

The Test Cases for static angles of attack, static trailing-edge control surface deflections, and static upper-surface spoiler deflections are presented in Tables 3-5, respectively. The Test Case Number, the TDT Test Number, and Test Point Number are included. In the Test Case Number, S =static conditions, T = trailing edge control surface, and U = upper surface spoiler. The test conditions are listed are the actual values from the data files. A listing of a sample of one of the static data files illustrating the format is given in Fig 6. For each pressure transducer, the time-averaged mean, the minimum value, the maximum value, and the standard deviation of the pressure coefficient is listed (these are generally called the channel statistics). An example of an application of the BACT data is given in Fig 7. Static pressures are shown for $\alpha = 4^{\circ}$ and $\delta_{te} = -10^{\circ}$ at both M = 0.65 and M = 0.75, and are compared with linear theory aerodynamics (Ref 31-32 for example). Significant transonic effects are shown at the higher Mach number over the forward portion of the chord. One feature of the BACT data set is an irregular pressure distribution at the spoiler hinge line that can be seen in Fig 7b. This feature is possibly related to the geometric details of the hinge line area or to a small flow through the hinge line.

The Test Cases for harmonic oscillation of the trailing edge control surface are given in Table 6, and for upper spoiler oscillations in Table 7. In the Test Case Number, O = harmonic oscillation, and again T = trailing edge control surface, and U = upper surface spoiler. There was no provision for oscillating the main wing and no Test Cases are included for an open lower surface spoiler. There are also no Test Cases included for both spoilers open. A listing of a sample of a data file for an oscillating trailing edge control case illustrating the format is given in Fig 8. The mean, minimum, maximum, and standard deviation are listed with the real and imaginary parts of the first harmonic of the unsteady pressures. The unsteady pressures are referenced to pitch displacement. The minimum, maximum, and standard deviation include the unsteady components and thus their interpretation is not straightforward. Measured pressure data for Test Case 8EOT31, a trailing edge control surface oscillation case, are shown in Fig 9. Large unsteady pressure components are evident both near the hinge line at x/c of 0.75, and at the shock located near x/c of 0.30.

The flutter conditions are shown in Fig 10 in terms of dynamic pressure versus Mach number and for zero control surface deflections. The classical flutter boundary is shown as a conventional boundary with Mach number with a minimum near M = 0.77, and a subsequent rise. Both the classical flutter boundary and the plunge instability are at small angles of attack, but the stall flutter points are at angles of attack of the order of 5°. Thus α is an independent variable for stall flutter that is not shown in Fig 10. The plunge instability occurs near zero lift, and it was found that opening the upper spoiler a small amount would suppress it. Earlier investigations could go around it by going to a higher angle of attack. Cases for all three types of flutter are selected and are listed in Table 8. In the Test Case Number, F = flutter, C =classical, S = stall, and P = plunge. The majority of the flutter points are included as Test Cases, except for nearly coincident points. For the flutter cases, calculations for flutter can be made and compared with measured boundaries. However, the model can also be forced to duplicate the measured combined pitch and plunge motions and the pressures compared directly. Only first harmonics are included in the data set, but time histories have been archived. In addition some cases are included for dynamic response measurements on the PAPA mount during forced oscillations of the control surfaces and are presented in Tables 9 and 10. In the Test Case Number, R = response, T = trailing edge control surface, and U = upper surface spoiler. Again calculations can be made including the structural response, or using the measured motion. The data file format for the flutter and response measurements is identical in format to

the files for the oscillating controls (Fig 8) except that the line for mean aerodynamic coefficients from the balance is replaced by the measured values of pitch and plunge displacement.

The unsteady pressures presented and included in the files have not been normalized by amplitude of motion. Case to case comparisons of pressures may need to be normalized by the pitch, plunge, or control surface amplitude value listed with the Test Case. For instances of pressures transducers malfunction, the pressures are set to zero.

The files included on the CD-ROM are ascii files and a readme file is included. There are separate files for each type of static and dynamic data organized in the manner of Tables 3-10. The file for static angle of attack is bactsa, for static trailing edge control is bactste, and for upper spoiler deflection is bactsus. A Fortran subprogram to read the static files, bactrdst.f, is included. The static data include the averaged pressures along with the mean, maximum and standard deviation for each channel of data. The data for oscillating control surfaces are on files bactdteo, and bactduso and the subprogram to read these files is bactrdos.f. The flutter and dynamic response data are on files bactdflt, bactdfter, and bactdfusr and the subprogram to read the files is bactftrd.f. The data files consist of contiguous data points. The measured ordinates are included on file bactorde.

Note that all of the data included for BACT were conducted with the heavy gas, R-12, as the test medium. The ratio of specific heats, γ, is calculated to be 1.132 to 1.135 for the conditions of the test assuming 0.99 for the fraction of heavy gas in the heavy gas-air mixture. A value of 1.132 is suggested for use in computational comparisons. The corresponding value of Prandtl number is calculated to range from 0.77 to 0.78 for the test conditions. For some cases, the calculated values of γ and Prandl number are included in the data files.

FORMULARY

1 General Description of Model

1.1	Designation	Benchmark Active Controls Technology Model (BACT)
1.2	Type	Semispan wing
1.3	Derivation	Same airfoil and planform as Benchmark NACA 0012/PAPA model (see Introduction)
1.4	Additional remarks	Overall view given in Fig 1 and shown mounted in tunnel in Fig 2
1.5	References	Ref 8 describes tests and data

2 Model Geometry

2.1	Planform	Rectangular
2.2	Aspect ratio	2.0 for the panel (neglecting tip of rotation)
2.3	Leading edge sweep	Unswept
2.4	Trailing edge sweep	Unswept
2.5	Taper ratio	1.0
2.6	Twist	None
2.7	Wing centreline chord	16 inches (406.4 mm)
2.8	Semi-span of model	32 inches (812.8 mm) plus tip of rotation
2.9	Area of planform	512 sq. in. (0.3303 sq. m) neglecting tip
2.10	Location of reference sections and definition of profiles	NACA 0012 airfoil throughout except for flat spoiler surfaces. Measured ordinates available as an electronic file
2.11	Lofting procedure between reference sections	Constant design airfoil section
2.12	Form of wing-body junction	No fairing and plate overlapped at splitter plate
2.13	Form of wing tip	Tip of rotation
2.14	Control surface details	Trailing edge control surface of 25% chord between 45% span and 75% span. Circular leading edge with hinge line not sealed, but a gap of less than .016 in (0.40 mm) between the spoiler trailing edge and the trailing edge control leading edge. Side edges open with a gap of the order of .031 in (0.80 mm). Upper and lower surface spoilers of 15% chord, hinged at 60% chord, and also running between 45% span and 75% span
2.15	Additional remarks	See Fig 1 for overview
2.16	References	Ref 8

3 Wind Tunnel

3.1	Designation	NASA LaRC Transonic Dynamics Tunnel (TDT)

3.2	Type of tunnel	Continuous flow, single return
3.3	Test section dimensions	16 ft x 16 ft (4.064 x 4.064 m)
3.4	Type of roof and floor	Three slots each
3.5	Type of side walls	Two sidewall slots
3.6	Ventilation geometry	Constant width slots in test region
3.7	Thickness of side wall boundary layer	Model tested on large splitter plate set out approximately 40 inches (1.02 m) from tunnel side wall (see Fig 2). Some documentation of tunnel wall boundary layer in Ref 18. Some results for the boundary layer on the splitter plate are presented in Ref 27
3.8	Thickness of boundary layers at roof and floor	Not documented
3.9	Method of measuring velocity	Calculated from static pressures measured in plenum and total pressure measured upstream of entrance nozzle of test section
3.10	Flow angularity	Not documented, considered small
3.11	Uniformity of velocity over test section	Not documented, considered nearly uniform, some nonuniformity over splitter plate above M = 0.80
3.12	Sources and levels of noise or turbulence in empty tunnel	Generally unknown. Some low speed measurements are presented in Ref 26. Cone transition measurements are presented in Ref 24 and 25.
3.13	Tunnel resonances	Unknown
3.14	Additional remarks	Tests performed in heavy gas, R-12. Ratio of specific heats, γ, is 1.132-1.135. For computations, 1.132 is recommended. For the conditions of this test, the Prandtl number is calculated to be 0.77-0.78
3.15	References on tunnel	Ref 18-20

4 Model Motion

4.1	General description	Oscillations about hinge line of control surfaces, and dynamic response and flutter on PAPA
4.2	Reference coordinate and definition of motion	Unswept hinge lines, see Fig 1 for conventions
4.3	Range of amplitude	Trailing edge control surface oscillation of 1, 2, and 4 degrees, spoiler up to 10 degrees
4.4	Range of frequency	Generally 0 to 10 Hz
4.5	Method of applying motion	Control surface oscillations driven by miniature hydraulic actuators at control surfaces. Flutter self excited or by control surface
4.6	Timewise purity of motion	Not documented
4.7	Natural frequencies and normal modes of model and support system	See Table 1 for plunge and pitch on PAPA. For higher modes see Ref 30. Not documented for rigid strut and balance
4.8	Actual mode of applied motion including any elastic deformation	Combined pitch and plunge measured for flutter and control surface rotations measured. Very stiff model with flutter below 5 Hz and control surface oscillations below 10 Hz and next vertical mode at 37 Hz
4.9	Additional remarks	None

5 Test Conditions

5.1	Model planform area/tunnel area	.015
5.2	Model span/tunnel height	.17
5.3	Blockage	Model less than 0.2% but splitter plate and equipment fairing is near 4%
5.4	Position of model in tunnel	Mounted from large splitter plate out from wall and on the tunnel centerline, Fig 2

5.5	Range of Mach number	0.63 to 0.94
5.6	Range of tunnel total pressure	Approximately 500 to 1000 psf (24 to 48 kPa)
5.7	Range of tunnel total temperature	512 to 576 degrees Rankinc (23 to 47° C)
5.8	Range of model steady or mean incidence	-4° to 10° pitch, 0 to 40° spoiler deflection, and -10° to 12° trailing edge control surface deflection
5.9	Definition of model incidence	From chord line of symmetric airfoil
5.10	Position of transition, if free	Transition strip used
5.11	Position and type of trip, if transition fixed	Grit strip at 5% chord on upper and lower surfaces.
5.12	Flow instabilities during tests	None defined
5.13	Changes to mean shape of model due to steady aerodynamic load	Not measured but considered very stiff
5.14	Additional remarks	Tests performed in heavy gas, R-12. Ratio of specific heats, γ, is 1.132-1.135. For computations, 1.132 is recommended. For the conditions of this test, the Prandtl number is calculated to be 0.77-0.78
5.15	References describing tests	Ref 8

6 Measurements and Observations

6.1	Steady pressures for the mean conditions	yes
6.2	Steady pressures for small changes from the mean conditions	yes
6.3	Quasi-steady pressures	no
6.4	Unsteady pressures	yes
6.5	Steady section forces for the mean conditions by integration of pressures	no
6.6	Steady section forces for small changes from the mean conditions by integration	no
6.7	Quasi-steady section forces by integration	no
6.8	Unsteady section forces by integration	no
6.9	Measurement of actual motion at points of model	yes
6.10	Observation or measurement of boundary layer properties	no
6.11	Visualisation of surface flow	no
6.12	Visualisation of shock wave movements	no
6.13	Additional remarks	no

7 Instrumentation

7.1	Steady pressure	
7.1.1	Position of orifices spanwise and chordwise	58 locations at 60% span and 17 at 40% span. See Figs 1 and 4
7.1.2	Type of measuring system	Used same transducers as unsteady pressure measurements
7.2	Unsteady pressure	
7.2.1	Position of orifices spanwise and chordwise	Same transducers as steady measurements. . See Figs 1 and 4
7.2.2	Diameter of orifices	.020 inches (.51 mm)
7.2.3	Type of measuring system	In situ pressure gages
7.2.4	Type of transducers	Kulites
7.2.5	Principle and accuracy of calibration	Statically calibrated and monitored through reference tubes
7.3	Model motion	
7.3.1	Method of measuring motion reference coordinate	Undocumented
7.3.2	Method of determining spatial mode of motion	Wind-off verification with accelerometers

7.3.3	Accuracy of measured motion	Undocumented
7.4	Processing of unsteady measurements	
7.4.1	Method of acquiring and processing measurements	Analog signals digitized at 500 samples/sec for 8-30 seconds depending on data type
7.4.2	Type of analysis	Fourier analysis
7.4.3	Unsteady pressure quantities obtained and accuracies achieved	Amplitude and phase of each pressure signal. Accuracy not specified
7.4.4	Method of integration to obtain forces	None
7.5	Additional remarks	None
7.6	References on techniques	Data system for test similar to one described in Ref 22

8 Data Presentation

8.1	Test Cases for which data could be made available	See Ref 8
8.2	Test Cases for which data are included in this document	See Tables 3-10
8.3	Steady pressures	Available for each Test Case
8.4	Quasi-steady or steady perturbation pressures	Steady pressures measured for several angles of attack
8.5	Unsteady pressures	Primary data is C_p mean, magnitude and phase for first harmonic only. Time histories have been archived
8.6	Steady forces or moments	5 component force balance used for static force measurements
8.7	Quasi-steady or unsteady perturbation forces	None
8.8	Unsteady forces and moments	None
8.9	Other forms in which data could be made available	None
8.10	Reference giving other representations of data	Ref 8-17

9 Comments on Data

9.1	Accuracy	
9.1.1	Mach number	Not documented
9.1.2	Steady incidence	Unknown
9.1.3	Reduced frequency	Should be accurate
9.1.4	Steady pressure coefficients	Not documented
9.1.5	Steady pressure derivatives	None
9.1.6	Unsteady pressure coefficients	Each gage individually calibrated and monitored statically through reference tube
9.2	Sensitivity to small changes of parameter	None indicated. Amplitudes of oscillation varied in test
9.3	Non-linearities	Many flow conditions involve shock waves and some with separation
9.4	Influence of tunnel total pressure	Not evaluated. Most of the test at constant dynamic pressure
9.5	Effects on data of uncertainty, or variation, in mode of model motion	Unknown, not expected to be appreciable
9.6	Wall interference corrections	None applied
9.7	Other relevant tests on same model	None
9.8	Relevant tests on other models of nominally the same shapes	Flutter tests on similar planform on PAPA presented in Ref 3-5
9.9	Any remarks relevant to comparison between experiment and theory	Some included under Model and Tests. Reynolds number included for each Test Case
9.10	Additional remarks	Reduced frequency based on root semichord of 8 inches (203.2 mm)
9.11	References on discussion of data	Ref 1-2 and 8-12

10 Personal Contact for Further Information

Head, Aeroelasticity Branch
Mail Stop 340
NASA Langley Research Center
Hampton, VA 23681-2199 USA

Phone: +1-(757)-864-2820
FAX: +1-(757)-864-8678

11 List of references

1. Bennett, Robert M.; Eckstrom, Clinton V.; Rivera, Jose, A.; Dansberry, Bryan E.; Farmer, Moses G.; and Durham, Michael H.: *The Benchmark Aeroelastic Models Program - Description and Highlights of Initial Results.* Paper No. 25 in Transonic Unsteady Aerodynamics and Aeroelasticity, AGARD CP 507, Mar. 1992. Also available as NASA TM-104180, 1991.

2. Durham, Michael H.; Keller, Donald F.; Bennett, Robert M.; and Wieseman, Carol D.: *A Status Report on a Model for Benchmark Active Controls Testing.* AIAA Paper 91-1011, Apr. 1991. Also available as NASA TM 107582, 1991.

3. Rivera, Jose A., Jr.; Dansberry, Bryan E.; Durham, Michael, H.; Bennett, Robert M.; and Silva, Walter A.: *Pressure Measurements on a Rectangular Wing with A NACA 0012 Airfoil During Conventional Flutter.* NASA TM 104211, July 1992.

4. Rivera, Jose A.; Dansberry, Bryan E.; Bennett, Robert M.; Durham, Michael, H.; and Silva, Walter A.: *NACA 0012 Benchmark Model Experimental Flutter Results with Unsteady Pressure Distributions.* AIAA Paper 92-2396, Apr. 1992. Also available as NASA TM 107581, Mar. 1992.

5. Rivera, Jose A.; Dansberry, Bryan E.; Farmer, Moses G.; Eckstrom, Clinton, V.; Seidel, David A.; and Bennett, Robert M.: *Experimental Flutter Boundaries with Unsteady Pressure Distributions for the NACA 0012 Benchmark Model.* AIAA 91-1010, 1991. Also available as NASA TM 104072, 1991.

6. Perry, Boyd, III; Cole, Stanley R.; and Miller, Gerald D.: *Summary of an Active Flexible Wing Program.* Journal of Aircraft, vol. 32, no. 1, Jan.-Feb. 1995, pp 10-15.

7. Sandford, Maynard C.; Abel, Irving; and Gray, David L.: *Development and Demonstration of a Flutter-Suppression System Using Active Controls.* NASA TR R-450, 1974.

8. Scott, Robert C.; Hoadley, Sherwood T.; Wieseman, Carol D.; and Durham, Michael H.: *The Benchmark Active Controls Technology Model Aerodynamic Data.* AIAA Paper 97-0829, Jan. 1997.

9. Bartels, R. E.; and Schuster, David M.: *A Comparison of Two Navier-Stokes Aeroelastic Methods Using BACT Benchmark Experimental Data.* AIAA Paper 99-3157, June 1999.

10. Schuster, David M.; Beran, Philip S.; and Huttsell, Lawrence J.: *Application of the ENS3DAE/Navier-Stokes Aeroelastic Method.* Paper No. 3 in Numerical Unsteady Aerodynamics and Aeroelastic Simulation, AGARD Report 822, Mar. 1998.

11. Roughen, K. M.; Baker, M. L.; and Fogarty T.: *CFD and Doublet-Lattice Calculation of Unsteady Control Surface Aerodynamics and Correlation with Wind Tunnel Test.* AAIA Paper 99-1469, Jan. 1999.

12. Waszak, Martin R.: *Modeling the Benchmark Active Control Technology Wind-Tunnel Model for Active Control Design Applications.* NASA/TP-1998-206270, June 1998.

13. Waszak, Martin R.: *Modeling the Benchmark Active Controls Technology Wind-Tunnel Model for Application to Flutter Suppression.* AIAA 96-3437, July 1996.

14. Waszak, Marty R. and Fung, James: *Parameter Identification and Analysis of Actuators for the BACT Wind-Tunnel Model.* AIAA Paper 96-3362, July 1996.

15. Lichtenwalner, P.; Little, G.; and Scott, R.: *Adaptive Neural Control of Aeroelastic Response.* SPIE 1996 Symposium on Smart Structures and Materials, San Diego, CA, Feb. 1996.

16. Lichtenwalner, P.; Little, G.; Pado, L.; and Scott, R.: *Adaptive Neural Control for Active Flutter Suppression.* SPIE 1997 Symposium on Smart Structures and Materials, San Diego, CA, Mar. 1997.

17. D'Cruz, Jonathan: A Determination of the External Forces Required to Move the Benchmark Active Controls Testing Model *in Pure Plunge and Pure Pitch.* NASA TM 107743, July 1993.

18. Aeroelasticity Branch Staff: The Langley Transonic Dynamics Tunnel. LWP-799, Sep. 1969.

19. Cole, Stanley, R.; and Rivera, Jose, A, Jr.: *The New Heavy Gas Testing Capability in the NASA Langley Transonic Dynamics Tunnel.* Paper No. 4, presented at the Royal Aeronautical Society Wind Tunnels and Wind Tunnel Test Techniques Forum, Churchill College, Cambridge, UK, Apr. 1997.

20. Corliss, James M.; and Cole, Stanley R.: *Heavy Gas Conversion of the NASA Langley Transonic Dynamics Tunnel.* AIAA Paper 98-2710, June 1998.

21. Cole, Patricia H.: *Wind Tunnel Real-Time Data Acquisition System.* NASA TM 80081, 1979.

22. Bryant, C.; and Hoadley, S. T.: *Open Architecture Dynamic Data System at Langley's Transonic Dynamics Tunnel.* AAIA Paper 98-0343, Jan. 1998.

23. Wieseman, Carol D.; and Hoadley, Sherwood, T.: *Versatile Software Package for Near Real-Time Analysis of Experimental Data.* AIAA Paper 98-2722, June 1999.

24. Dougherty, N. Sam, Jr.: *Influence of Wind Tunnel Noise on the Location of Boundary-Layer Transition on a Slender Cone at Mach Numbers from 0.2 to 5.5. Volume I. - Experimental Methods and Summary of Results. Volume II. - Tabulated and Plotted Data.* AEDC--TR-78-44, March 1980.

25. Dougherty, N. Sam, Jr.; and Fisher, D. F.: *Boundary-Layer Transition on a 10-Deg. Cone: Wind Tunnel/Flight Correlation.* AIAA Paper 80-0154, Jan. 1980.

26. Sleeper, Robert K.; Keller, Donald F.; Perry, Boyd, III; and Sandford, Maynard C.: *Characteristics of Vertical and Lateral Tunnel Turbulence Measured in Air in the Langley Transonic Dynamics Tunnel.* NASA TM 107734, March 1993.

27. Schuster, David M: *Aerodynamic Measurements on a Large Splitter Plate for the NASA Langley Transonic Dynamics Tunnel.* Proposed NASA TM, 1999.

28. Farmer, Moses G.: *A Two-Degree-of-Freedom Flutter Mount System with Low Damping for Testing Rigid Wings at Different Angles of Attack. NASA* TM 83302, 1982.

29. Farmer, Moses G.: *Mount System for Testing Flutter.* U.S Patent No. 4,475,385, Oct. 9, 1984.

30. Dansberry, Bryan E.; Durham, Michael, H.; Bennett, Robert M.; Turnock, David L.; Silva, Walter A.; and Rivera, Jose A., Jr.: *Physical Properties of the Benchmark Models Program Supercritical Wing.* NASA TM 4457, Sep. 1993.

31. Rowe, W. S.; Redman, M. C.; Ehlers, F. E.; and Sebastian, J. D.: *Prediction of Unsteady Aerodynamic Loadings Caused by Leading Edge and Trailing Edge Control Surface Motions in Subsonic Compressible Flow—Analysis and Results.* NASA CR-2543, May 1975.

32. Giesing, J. P.; Kalman, T. P.; and Rodden, W. P.: *Subsonic Unsteady Aerodynamics for General Configurations, Part I – Vol. I – Direct Application of the Nonplanar Doublet Lattice Method.* AFFDL-TR-71-5, Nov. 1971.

Table 1. Measured Nominal Structural Dynamic Parameters

	Plunge Mode	Pitch Mode
Frequency	3.34 Hz.	5.21 Hz.
Stiffness	2,686 lb/ft	3,000 ft-lb/rad
Damping Ratio, ζ	0.0014	0.0010
Effective Mass or Inertia	6.08 slug	2.80 slug-ft^2

Table 2. Instrumentation

Instrument	Quantity
Model Pressure Transducers	75
Splitter Plate Pressure Transducers (Test 485 only)	20
Boundary Layer Rake Pressure Transducers (Test 485 only)	10
Model Accelerometers	4
Control Surface Accelerometers	6
Control Surface Potentiometers	3
Control Surface Command Signals	3
Hydraulic Pressure Transducers	6
Balance Components (Rigid support only)	5
PAPA Strain Gage Bridges (Flexible support only)	2
PAPA Accelerometers (Flexible support only)	2
Turntable AOA Accelerometer	1
Model AOA Accelerometer	1

Table 3. Static Test Cases for Angle Of Attack

Test Case No.	Test	Run	Point No.	M	q psf	α deg.	δ_{te_0} deg.	δ_{us_0} deg.	δ_{ls_0} deg.	Wind-Off Zero Point No.
8ESA1	485	27	1911	0.650	145.0	-0.03	0.3	0.2	0.2	1910
8ESA2	485	27	1912	0.648	144.2	0.51	0.3	0.2	0.2	1910
8ESA3	485	27	1913	0.650	144.8	1.01	0.3	0.2	0.2	1910
8ESA4	485	27	1914	0.650	145.1	2.05	0.3	0.2	0.2	1910
8ESA5	485	27	1915	0.649	144.6	3.99	0.3	0.2	0.2	1910
8ESA6	485	27	1916	0.651	145.3	6.01	0.3	0.2	0.2	1910
8ESA7	485	27	1917	0.650	145.1	-2.01	0.3	0.2	0.2	1910
8ESA8	485	27	1918	0.649	144.8	-4.01	0.3	0.2	0.2	1910
8ESA9	485	5	136	0.768	140.4	-0.01	0.0	0.2	0.0	132
8ESA10	485	5	137	0.771	141.6	0.51	0.0	0.2	0.0	132
8ESA11	485	5	138	0.772	142.1	1.01	0.0	0.2	0.0	132
8ESA12	485	5	139	0.769	141.6	2.00	0.0	0.2	0.0	132
8ESA13	485	5	140	0.769	141.7	3.01	0.0	0.2	0.0	132
8ESA14	485	5	141	0.768	141.5	3.99	0.0	0.2	0.0	132
8ESA15	485	5	142	0.769	141.7	5.00	0.0	0.2	0.0	132
8ESA16	485	5	143	0.770	142.3	6.01	0.0	0.2	0.0	132
8ESA17	485	5	144	0.768	141.7	7.02	0.0	0.2	0.0	132
8ESA18	485	5	145	0.769	142.2	8.02	0.0	0.2	0.0	132
8ESA19	485	5	146	0.769	142.2	9.00	0.0	0.1	0.0	132
8ESA20	485	5	147	0.770	142.6	6.02	0.0	0.2	0.0	132
8ESA21	485	5	148	0.769	142.6	4.02	0.0	0.2	0.0	132
8ESA22	485	5	150	0.769	142.8	-0.03	0.0	0.1	0.0	132
8ESA23	485	5	151	0.769	142.8	-2.02	0.0	0.1	0.0	132
8ESA24	485	5	152	0.769	142.9	-4.02	0.0	0.1	0.0	132
8ESA25	485	21	1405	0.821	169.2	-0.01	0.3	0.2	0.2	1404
8ESA26	485	21	1406	0.817	168.5	0.50	0.3	0.2	0.2	1404
8ESA27	485	21	1407	0.817	168.5	1.03	0.3	0.2	0.2	1404
8ESA28	485	21	1408	0.819	169.0	2.05	0.3	0.2	0.2	1404
8ESA29	485	21	1409	0.819	169.1	3.12	0.3	0.2	0.2	1404
8ESA30	485	21	1410	0.821	169.9	3.99	0.3	0.2	0.2	1404
8ESA31	485	21	1411	0.819	169.5	5.01	0.3	0.2	0.2	1404
8ESA32	485	21	1412	0.819	169.4	6.00	0.3	0.2	0.2	1404
8ESA33	485	21	1413	0.819	169.4	7.04	0.3	0.2	0.2	1404
8ESA34	485	21	1414	0.820	169.7	8.04	0.3	0.1	0.2	1404
8ESA35	485	21	1415	0.819	169.6	9.04	0.3	0.1	0.2	1404
8ESA36	485	21	1416	0.819	169.8	10.04	0.3	0.1	0.2	1404
8ESA37	485	21	1418	0.816	169.2	6.01	0.3	0.2	0.2	1404
8ESA38	485	21	1420	0.818	169.7	1.99	0.3	0.2	0.2	1404
8ESA39	485	21	1421	0.818	169.8	-0.06	0.3	0.2	0.2	1404
8ESA40	485	21	1423	0.818	169.8	-4.01	0.3	0.2	0.2	1404
8ESA41	485	25	1715	0.902	134.5	0.00	0.2	0.3	0.1	1714
8ESA42	485	25	1716	0.903	134.7	0.26	0.2	0.4	0.1	1714
8ESA43	485	25	1717	0.899	134.0	0.50	0.2	0.4	0.2	1714
8ESA44	485	25	1718	0.900	134.2	0.75	0.2	0.3	0.4	1714
8ESA45	485	25	1719	0.902	134.7	1.02	0.2	0.3	0.4	1714
8ESA46	485	25	1720	0.897	133.9	1.52	0.2	0.4	0.5	1714
8ESA47	485	25	1721	0.899	134.4	2.00	0.2	0.3	0.4	1714
8ESA48	485	25	1722	0.896	133.9	3.01	0.2	0.3	0.4	1714

Table 4. Static Test Cases for Trailing Edge Control Surface Deflection

Test Case No.	Test	Run	Point No.	M	q psf	α deg.	δ_{te_0} deg.	δ_{us_0} deg	δ_{ls_0} deg	Wind-Off Zero Point No.
8EST1	485	27	1929	0.649	145.0	0.01	-9.7	0.2	0.2	1910
8EST2	485	27	1930	0.648	144.8	0.01	-4.8	0.2	0.4	1910
8EST3	485	27	1931	0.648	144.7	0.01	-1.7	0.2	0.2	1910
8EST4	485	27	1932	0.648	144.7	0.01	0.3	0.2	0.3	1910
8EST5	485	27	1933	0.650	145.4	0.01	2.3	0.2	0.3	1910
8EST6	485	27	1934	0.650	145.2	0.01	5.3	0.2	0.2	1910
8EST7	485	27	1935	0.651	145.6	0.01	10.3	0.2	0.2	1910
8EST8	485	27	1937	0.649	145.1	1.99	-9.8	0.2	0.1	1910
8EST9	485	27	1938	0.650	145.4	1.99	-4.8	0.2	0.2	1910
8EST10	485	27	1939	0.650	145.3	1.99	-1.7	0.2	0.1	1910
8EST11	485	27	1940	0.650	145.4	1.99	0.3	0.2	0.1	1910
8EST12	485	27	1941	0.650	145.6	1.99	2.3	0.2	0.2	1910
8EST13	485	27	1942	0.649	145.3	1.99	5.3	0.2	0.2	1910
8EST14	485	27	1943	0.649	145.3	1.99	10.3	0.2	0.2	1910
8EST15	485	5	156	0.767	142.9	0.03	-10.0	0.1	-0.1	132
8EST16	485	5	157	0.768	143.1	0.03	-5.0	0.1	-0.1	132
8EST17	485	5	158	0.771	143.9	0.03	-2.0	0.1	-0.1	132
8EST18	485	5	159	0.768	143.1	0.03	0.0	0.1	-0.1	132
8EST19	485	5	160	0.772	144.4	0.03	0.5	0.1	-0.1	132
8EST20	485	5	161	0.769	143.5	0.03	1.0	0.1	-0.1	132
8EST21	485	5	162	0.768	143.4	0.03	2.0	0.1	-0.1	132
8EST22	485	5	163	0.770	143.9	0.03	3.0	0.1	0.0	132
8EST23	485	5	164	0.769	143.7	0.03	5.0	0.1	0.0	132
8EST24	485	5	165	0.770	144.1	0.03	10.0	0.1	-0.1	132
8EST25	485	5	166	0.770	144.1	0.03	12.0	0.1	-0.1	132
8EST26	485	5	193	0.770	145.2	3.99	-9.9	0.1	-0.1	132
8EST27	485	5	195	0.769	145.1	3.99	-5.0	0.1	-0.1	132
8EST28	485	5	196	0.770	145.5	3.99	-1.9	0.1	-0.1	132
8EST29	485	5	197	0.769	145.3	3.99	0.0	0.1	-0.1	132
8EST30	485	5	200	0.768	145.1	3.99	1.0	0.1	-0.1	132
8EST31	485	5	201	0.769	145.3	3.99	2.0	0.1	-0.1	132
8EST32	485	5	202	0.770	145.6	3.99	3.0	0.1	-0.1	132
8EST33	485	5	203	0.769	145.4	3.99	5.0	0.1	-0.1	132
8EST34	485	5	204	0.769	145.4	3.99	10.0	0.1	-0.1	132
8EST35	485	5	205	0.770	145.6	3.99	12.0	0.1	-0.1	132

Table 4. Concluded

Test Case No.	Test	Run	Point No.	M	q psf	α deg.	δ_{te_0} deg.	δ_{us_0} deg.	δ_{ls_0} deg	Wind-Off Zero Point No.
8EST36	485	21	1425	0.818	170.0	0.03	-9.7	-0.2	0.2	1404
8EST37	485	21	1426	0.820	170.6	0.03	-4.7	-0.1	0.2	1404
8EST38	485	21	1427	0.818	170.0	0.03	-1.7	-0.1	0.2	1404
8EST39	485	21	1428	0.817	170.0	0.03	0.3	-0.1	0.2	1404
8EST40	485	21	1429	0.820	170.7	0.03	1.3	-0.1	0.2	1404
8EST41	485	21	1430	0.819	170.5	0.03	2.3	-0.1	0.2	1404
8EST42	485	21	1431	0.818	170.3	0.03	3.3	-0.1	0.2	1404
8EST43	485	21	1432	0.817	170.0	0.03	5.3	-0.1	0.2	1404
8EST44	485	21	1433	0.818	170.3	0.03	10.3	-0.1	0.2	1404
8EST45	485	21	1434	0.821	171.1	0.03	12.3	-0.1	0.2	1404
8EST46	485	21	1447	0.817	170.3	4.01	-9.7	-0.1	0.2	1404
8EST47	485	21	1448	0.819	170.9	4.01	-4.7	-0.1	0.2	1404
8EST48	485	21	1449	0.818	170.8	4.01	-1.7	-0.1	0.2	1404
8EST49	485	21	1450	0.817	170.5	4.01	0.3	-0.1	0.2	1404
8EST50	485	21	1451	0.817	170.7	4.01	1.3	-0.1	0.2	1404
8EST51	485	21	1452	0.818	170.9	4.01	2.3	-0.1	0.2	1404
8EST52	485	21	1453	0.818	170.9	4.01	3.4	-0.1	0.2	1404
8EST53	485	21	1454	0.817	170.5	4.01	5.4	-0.1	0.2	1404
8EST54	485	21	1455	0.816	170.3	4.01	10.3	-0.1	0.2	1404
8EST55	485	21	1456	0.818	170.8	4.00	12.3	-0.1	0.2	1404
8EST56	485	25	1735	0.896	134.9	-0.05	-4.8	0.3	0.3	1714
8EST57	485	25	1737	0.899	135.6	-0.05	-1.7	0.2	0.3	1714
8EST58	485	25	1738	0.896	135.2	-0.05	-0.7	0.2	0.3	1714
8EST59	485	25	1739	0.896	135.2	-0.05	-0.3	0.2	0.3	1714
8EST60	485	25	1740	0.897	135.3	-0.05	0.3	0.2	0.3	1714
8EST61	485	25	1741	0.897	135.4	-0.05	0.7	0.2	0.3	1714
8EST62	485	25	1742	0.898	135.5	-0.05	1.3	0.2	0.3	1714
8EST63	485	25	1745	0.897	135.7	-0.05	1.8	0.2	0.2	1714
8EST64	485	25	1746	0.899	136.0	-0.05	2.2	0.2	0.1	1714
8EST65	485	25	1747	0.901	136.4	-0.05	5.2	0.3	0.1	1714

Table 5. Static Test Cases for Upper Spoiler Deflection

Test Case No.	Test	Run	Point No.	M	q psf	α deg.	δ_{te_0} deg.	δ_{us_0} deg.	δ_{ls_0} deg.	Wind-Off Zero Point No.
8ESU1	485	27	1953	0.648	145.0	0.00	0.2	0.2	0.2	1910
8ESU2	485	27	1954	0.649	145.3	0.00	0.2	-4.8	0.2	1910
8ESU3	485	27	1955	0.649	145.5	0.00	0.2	-9.8	0.2	1910
8ESU4	485	27	1956	0.648	144.9	0.00	0.2	-20.0	0.2	1910
8ESU5	485	27	1957	0.649	145.4	0.00	0.2	-40.1	0.2	1910
8ESU6	485	27	1959	0.649	145.6	3.98	0.2	0.3	0.2	1910
8ESU7	485	27	1960	0.647	145.0	3.98	0.2	-4.8	0.2	1910
8ESU8	485	27	1961	0.649	145.4	3.98	0.2	-9.8	0.2	1910
8ESU9	485	27	1962	0.649	145.6	3.98	0.2	-19.9	0.2	1910
8ESU10	485	27	1963	0.649	145.5	3.98	0.2	-40.2	0.2	1910
8ESU11	485	8	361	0.771	146.4	-0.01	0.0	-0.2	0.0	360
8ESU12	485	8	362	0.775	146.7	-0.01	0.0	-0.5	0.0	360
8ESU13	485	8	363	0.772	146.0	-0.01	0.0	-0.5	0.0	360
8ESU14	485	8	364	0.772	145.9	-0.01	0.1	-1.0	0.0	360
8ESU15	485	8	365	0.770	145.6	-0.01	0.1	-2.0	0.0	360
8ESU16	485	8	366	0.770	145.6	-0.01	0.1	-5.0	0.0	360
8ESU17	485	8	367	0.772	146.3	-0.01	0.0	-9.9	0.0	360
8ESU18	485	8	368	0.769	145.5	-0.01	0.0	-15.0	0.0	360
8ESU19	485	8	369	0.770	146.0	-0.01	0.0	-20.0	0.0	360
8ESU20	485	8	370	0.770	146.0	-0.01	0.0	-25.0	0.0	360
8ESU21	485	8	371	0.772	146.9	-0.02	0.0	-35.1	0.0	360
8ESU22	485	21	1458	0.817	171.0	-0.02	0.3	-0.1	0.1	1404
8ESU23	485	21	1459	0.816	170.6	-0.03	0.3	-0.9	0.2	1404
8ESU24	485	21	1460	0.819	171.3	-0.03	0.3	-2.0	0.2	1404
8ESU25	485	21	1461	0.818	171.4	-0.03	0.3	-4.9	0.2	1404
8ESU26	485	21	1462	0.820	171.8	-0.03	0.3	-10.0	0.2	1404
8ESU27	485	21	1463	0.818	171.2	-0.03	0.3	-14.9	0.2	1404
8ESU28	485	21	1464	0.817	171.0	-0.03	0.3	-19.8	0.2	1404
8ESU29	485	25	1775	0.899	137.2	-0.03	0.2	0.3	0.3	1714
8ESU30	485	25	1776	0.897	137.1	-0.03	0.3	-0.9	0.3	1714
8ESU31	485	25	1777	0.895	136.9	-0.03	0.2	-2.0	0.3	1714
8ESU32	485	25	1778	0.897	137.1	-0.03	0.3	-3.0	0.2	1714

Table 6. Test Cases for Trailing Edge Control Surface Oscillation, $\delta_{us_o} = 0$

Test Case No.	Test	Run	Point No.	M	q psf	α deg.	δ_{te_o} deg.	δ_{te} deg.	k	Frequency Hz	Wind-Off Zero Point No.
8EOT1	485	27	1966	0.648	145.3	0.04	0.25	4.05	0.0257	2.00	1910
8EOT2	485	27	1967	0.648	145.2	0.09	0.27	4.04	0.0645	5.01	1910
8EOT3	485	27	1968	0.647	145.1	0.05	0.27	3.83	0.1291	10.02	1910
8EOT4	485	27	1972	0.648	145.5	4.03	0.25	4.05	0.0257	2.00	1910
8EOT5	485	27	1973	0.647	145.1	4.02	0.27	4.04	0.0646	5.01	1910
8EOT6	485	27	1974	0.648	145.5	4.00	0.27	3.83	0.1289	10.02	1910
8EOT7	485	14	901	0.768	151.2	-0.03	0.05	1.07	0.1076	9.93	879
8EOT8	485	14	904	0.767	151.4	0.04	0.05	2.04	0.0108	1.00	879
8EOT9	485	14	905	0.768	151.6	-0.06	0.05	2.05	0.0217	2.00	879
8EOT10	485	14	906	0.769	152.0	0.07	0.05	2.05	0.0325	3.00	879
8EOT11	485	14	907	0.769	151.9	0.01	0.05	2.06	0.0431	3.99	879
8EOT12	485	14	908	0.766	151.2	0.04	0.05	2.07	0.0544	5.01	879
8EOT13	485	14	909	0.768	152.0	-0.06	0.06	2.08	0.0650	6.00	879
8EOT14	485	14	910	0.769	152.2	0.04	0.08	2.08	0.0868	8.03	879
8EOT15	485	14	911	0.768	151.8	-0.02	0.08	2.07	0.1076	9.93	879
8EOT16	485	14	916	0.770	152.6	0.13	0.08	3.00	0.1073	9.93	879
8EOT17	485	14	919	0.769	152.5	0.07	0.07	4.06	0.0216	2.00	879
8EOT18	485	14	920	0.769	152.6	0.10	0.08	4.06	0.0542	5.01	879
8EOT19	485	14	921	0.769	152.6	0.12	0.08	3.89	0.1074	9.93	879
8EOT20	485	14	933	0.769	153.3	-0.04	5.09	2.03	0.1073	9.93	879
8EOT21	485	14	936	0.768	153.1	-0.03	5.08	4.05	0.0216	2.00	879
8EOT22	485	14	937	0.768	153.1	-0.03	5.10	4.03	0.0542	5.01	879
8EOT23	485	14	938	0.768	153.0	-0.02	5.08	3.84	0.1075	9.93	879
8EOT24	485	16	1049	0.765	145.0	2.01	0.08	4.05	0.0218	2.00	963
8EOT25	485	16	1050	0.767	145.4	2.04	0.10	4.05	0.0544	5.01	963
8EOT26	485	16	1051	0.768	145.8	2.08	0.10	3.88	0.1086	10.02	963
8EOT27	485	17	1083	0.767	147.4	4.10	0.09	1.07	0.1088	10.02	1060
8EOT28	485	17	1088	0.768	148.0	4.04	0.09	2.05	0.1086	10.02	1060
8EOT29	485	17	1092	0.769	148.3	4.05	0.08	4.04	0.0217	2.00	1060
8EOT30	485	17	1093	0.768	148.3	4.15	0.10	4.04	0.0543	5.01	1060
8EOT31	485	17	1094	0.771	149.0	4.01	0.10	3.87	0.1083	10.02	1060
8EOT32	485	17	1121	0.767	148.7	4.99	0.08	4.04	0.0217	2.00	1060
8EOT33	485	17	1124	0.767	149.1	4.93	0.09	4.04	0.0543	5.01	1060
8EOT34	485	17	1126	0.767	149.2	5.08	0.10	3.87	0.1087	10.02	1060
8EOT35	485	18	1165	0.769	151.8	5.93	0.08	4.04	0.0217	2.00	1154
8EOT36	485	18	1166	0.770	152.2	5.87	0.10	4.04	0.0542	5.01	1154
8EOT37	485	18	1167	0.767	151.4	5.98	0.10	3.87	0.1088	10.02	1154
8EOT38	485	22	1557	0.818	175.2	0.02	0.04	4.04	0.0204	2.00	1519
8EOT39	485	22	1558	0.819	175.2	0.03	0.05	4.04	0.0510	5.01	1519
8EOT40	485	22	1560	0.819	175.4	0.06	0.06	3.88	0.1019	10.02	1519
8EOT41	485	22	1568	0.817	175.2	3.97	0.04	4.04	0.0204	2.00	1519
8EOT42	485	22	1569	0.817	175.1	3.97	0.06	4.04	0.0511	5.01	1519
8EOT43	485	22	1570	0.817	175.1	4.03	0.07	3.86	0.1022	10.02	1519
8EOT44	485	25	1789	0.900	138.5	-0.19	0.25	2.04	0.0186	2.00	1714
8EOT45	485	25	1790	0.899	138.3	-0.23	0.25	2.06	0.0466	5.01	1714
8EOT46	485	25	1791	0.898	138.2	-0.21	0.26	2.06	0.0934	10.02	1714
8EOT47	485	25	1798	0.898	138.4	0.34	0.26	2.05	0.0933	10.02	1714

Table 7. Test Cases for Upper Spoiler Oscillations, $\delta_{te_0} = 0$

Test Case No.	Test	Run	Point No.	M	q psf	α deg.	δ_{us_0} deg.	δ_{us} deg.	k	Frequency Hz	Wind-Off Zero Point No.
8EOU1	485	27	1978	0.648	145.5	-0.02	-9.86	2.12	0.0257	2.00	1910
8EOU2	485	27	1979	0.648	145.4	-0.02	-9.84	2.17	0.0645	5.01	1910
8EOU3	485	27	1980	0.647	145.3	-0.02	-9.82	2.29	0.1291	10.02	1910
8EOU4	485	27	1988	0.648	145.7	3.99	-10.60	2.17	0.0257	2.00	1910
8EOU5	485	27	1989	0.648	145.7	3.99	-10.58	2.21	0.0645	5.01	1910
8EOU6	485	27	1990	0.648	145.9	3.99	-10.54	2.37	0.1289	10.02	1910
8EOU7	485	18	1188	0.769	152.7	-0.01	-5.06	2.36	0.1085	10.02	1154
8EOU8	485	18	1197	0.770	153.1	-0.01	-5.01	4.47	0.1084	10.02	1154
8EOU9	485	18	1201	0.769	153.0	-0.01	-10.06	2.10	0.0216	2.00	1154
8EOU10	485	18	1202	0.769	153.0	-0.01	-10.04	2.16	0.0543	5.01	1154
8EOU11	485	18	1203	0.768	152.6	-0.01	-10.02	2.26	0.1087	10.02	1154
8EOU12	485	18	1207	0.769	153.2	-0.01	-10.09	10.44	0.1085	10.02	1154
8EOU13	485	18	1211	0.768	152.9	-0.01	-20.01	2.09	0.0217	2.00	1154
8EOU14	485	18	1212	0.768	153.0	-0.01	-20.00	2.05	0.0543	5.01	1154
8EOU15	485	18	1213	0.768	152.9	-0.01	-19.97	2.10	0.1086	10.02	1154
8EOU16	485	18	1217	0.769	153.4	-0.01	-19.65	10.18	0.1085	10.02	1154
8EOU17	485	20	1369	0.768	150.7	5.01	-19.52	10.25	0.1086	10.02	1298
8EOU18	485	22	1574	0.818	175.6	0.00	-9.94	2.15	0.0204	2.00	1519
8EOU19	485	22	1575	0.819	176.1	0.00	-9.93	2.18	0.0509	5.01	1519
8EOU20	485	22	1576	0.818	175.8	0.00	-9.90	2.27	0.1020	10.02	1519
8EOU21	485	22	1580	0.819	176.0	0.00	-10.09	10.36	0.1020	10.02	1519
8EOU22	485	22	1584	0.815	174.9	0.00	-19.89	2.11	0.0204	2.00	1519
8EOU23	485	22	1585	0.818	175.8	0.00	-19.89	2.08	0.0510	5.01	1519
8EOU24	485	22	1586	0.819	176.4	0.00	-19.84	2.14	0.1019	10.02	1519
8EOU25	485	22	1590	0.819	176.3	0.00	-19.43	10.15	0.1020	10.02	1519
8EOU26	485	23	1618	0.819	177.4	4.01	-19.51	10.26	0.1020	10.02	1608
8EOU27	485	25	1802	0.896	138.4	-0.01	-2.02	2.16	0.0187	2.00	1714

Table 8. BACT Flutter Test Cases

Test Case No.	Test	Run	Point No.	M	q psf	α deg.	Type	k	Flutter Freq., Hz	Wind-Off Zero Point No.
8EFC1	502	25	1438	0.631	158.2	1.64	Classical	0.0574	4.31	1379
8EFC2	502	25	1394	0.747	151.6	1.78	Classical	0.0470	4.14	1379
8EFC3	502	27	1524	0.770	145.2	1.72	Classical	0.0458	4.19	1484
8EFC4	502	26	1469	0.793	146.5	1.81	Classical	0.0439	4.13	1450
8EFC5	502	28	1685	0.801	151.7	2.09	Classical	0.0436	4.17	1569
8EFC6	502	26	1472	0.804	149.9	1.86	Classical	0.0430	4.10	1450
8EFC7	502	26	1477	0.842	161.1	1.83	Classical	0.0420	4.20	1450
8EFC8	502	25	1405	0.859	191.8	1.85	Classical	0.0408	4.10	1379
8EFP1	485	36	2324	0.928	163.7	-0.06	Plunge	0.0304	3.37	2300
8EFP2	485	41	2490	0.935	124.2	-0.06	Plunge	0.0299	3.31	2481
8EFP3	485	33	2240	0.937	133.8	0.03	Plunge	0.0294	3.27	2205
8EFP4	485	41	2488	0.939	124.7	-0.05	Plunge	0.0289	3.21	2481
8EFS1	485	43	2648	0.768	124.2	6.34	Stall	0.0520	4.77	2604
8EFS2	485	42	2571	0.799	126.9	5.43	Stall	0.0506	4.83	2543
8EFS3	485	36	2332	0.799	137.6	5.15	Stall	0.0497	4.74	2300

Table 9. Test Cases for Forced Response with Trailing Edge Control Surface on PAPA, $\delta_{us_o} = \delta_{te_o} = 0$

Test Case No.	Test	Run	Point No.	M	q psf	α deg.	δ_{te} deg.	k	Frequency Hz	Wind-Off Zero Point No.
8ERT1	485	38	2377	0.648	112.6	2.02	1.56	0.0445	3.45	2355
8ERT2	485	38	2380	0.649	113.0	2.02	4.08	0.0579	4.50	2355
8ERT3	485	43	2618	0.771	123.6	1.99	1.04	0.0374	3.44	2604
8ERT4	485	43	2619	0.770	123.4	1.98	2.07	0.0467	4.30	2604
8ERT5	485	42	2573	0.796	126.4	4.94	1.05	0.0492	4.69	2543
8ERT6	485	42	2551	0.798	125.0	2.09	2.06	0.0362	3.45	2543
8ERT7	485	42	2553	0.795	124.5	2.09	4.09	0.0456	4.32	2543
8ERT8	485	46	2723	0.875	129.5	2.02	1.04	0.0333	3.44	2718
8ERT9	485	46	2724	0.879	130.5	1.96	4.07	0.0450	4.69	2718

Table 10. Test Cases for Forced Response with Upper Surface Spoiler on PAPA, $\delta_{te_o} = 0$

Test Case No.	Test	Run	Point No.	M	q psf	α deg.	δ_{us_o} deg.	δ_{us} deg.	k	Frequency Hz	Wind-Off Zero Point No.
8ERU1	485	39	2434	0.649	116.3	1.89	-10.03	1.00	0.0452	3.50	2398
8ERU2	485	39	2435	0.649	115.7	1.90	-10.02	2.07	0.0582	4.50	2398
8ERU3	485	43	2630	0.768	123.5	1.92	-4.97	2.11	0.0375	3.44	2604
8ERU4	485	43	2631	0.770	124.0	1.93	-4.97	0.99	0.0469	4.32	2604
8ERU5	485	42	2587	0.799	127.7	5.24	-5.09	1.00	0.0504	4.81	2543
8ERU6	485	42	2562	0.795	125.6	2.04	-5.07	2.07	0.0382	3.63	2543
8ERU7	485	42	2563	0.800	126.7	2.02	-5.07	2.05	0.0452	4.32	2543
8ERU8	485	46	2729	0.873	130.2	1.99	-5.07	4.15	0.0332	3.44	2718
8ERU9	485	46	2730	0.874	130.3	2.00	-5.07	4.16	0.0452	4.69	2718

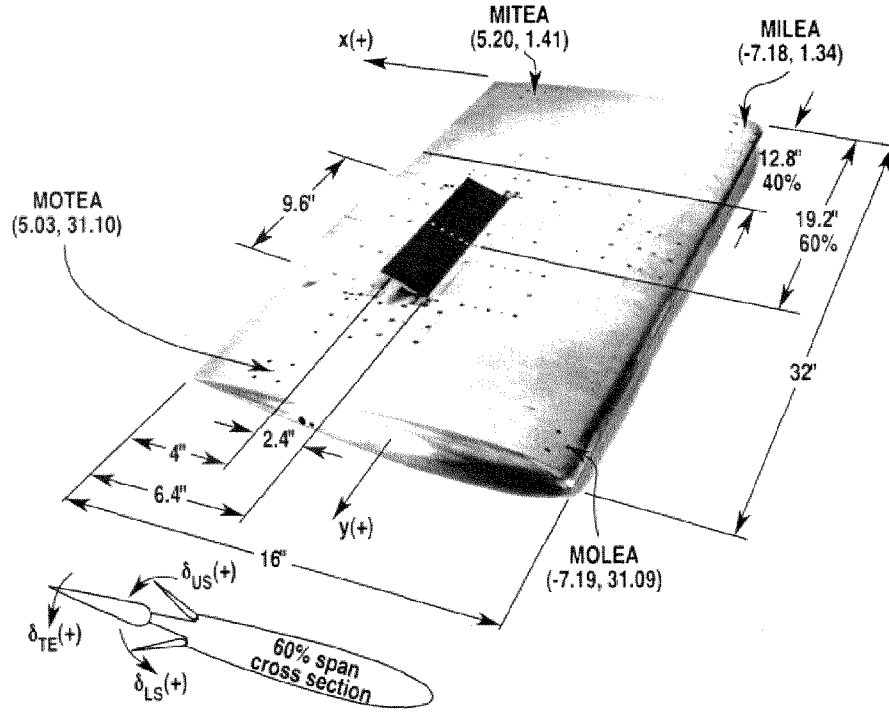

Figure 1. BACT model, dimensions in inches and origin at root midchord.

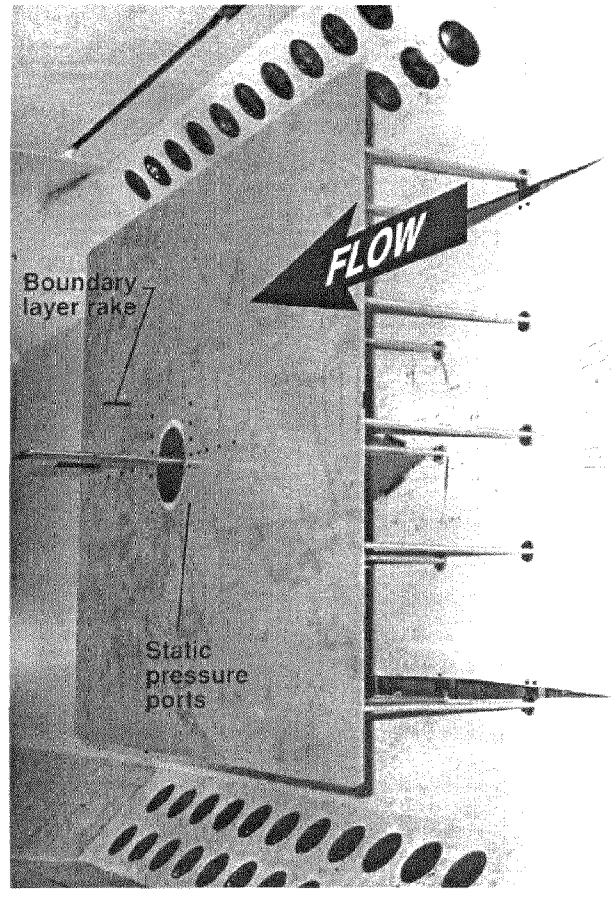

Figure 2. BACT model installed in Transonic Dynamics Tunnel

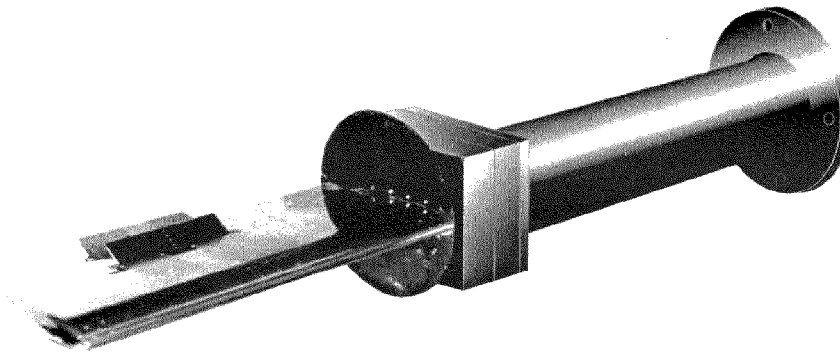

a) Model on the rigid mount (balance and strut).

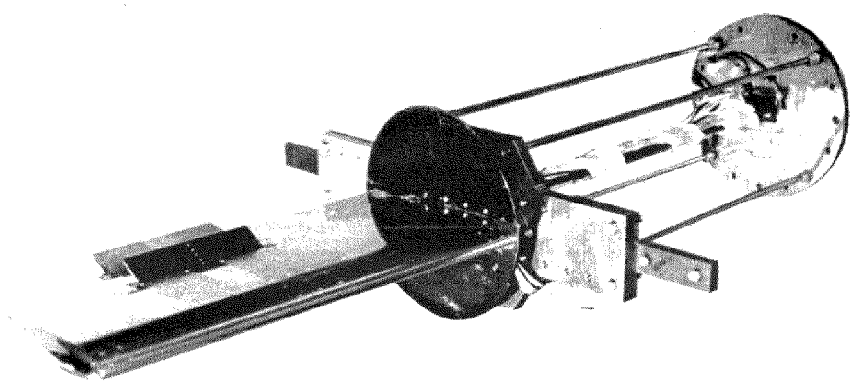

b) Model on the flexible mount (PAPA).

Figure 3. BACT model on rigid and flexible mount systems.

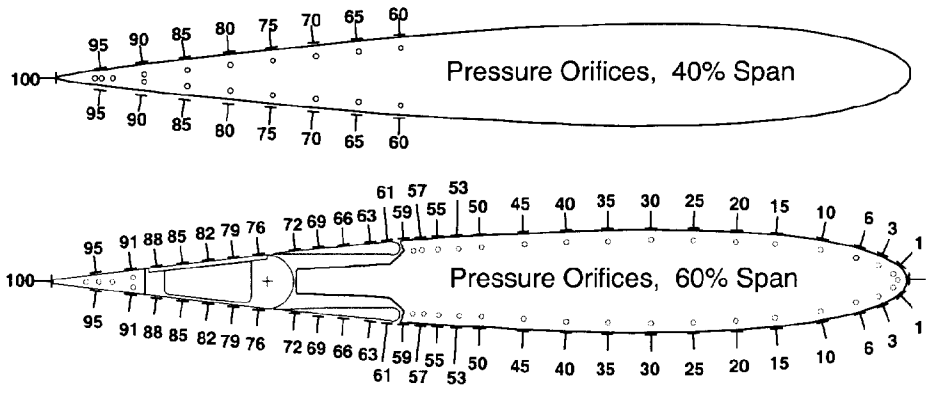

Figure 4. Pressure orifice locations, percent chord.

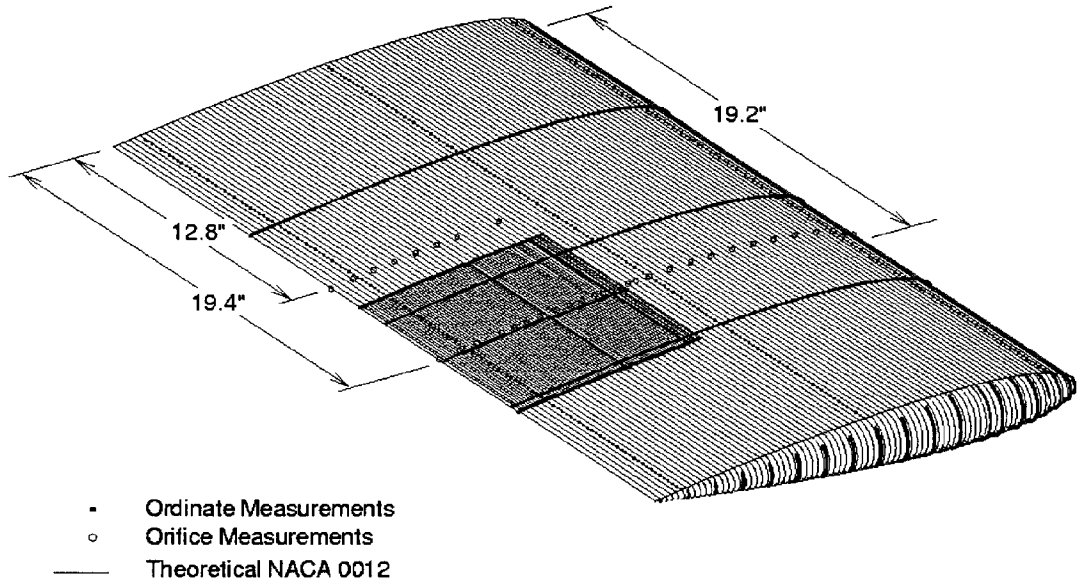

a) Ordinate measurements for entire model.

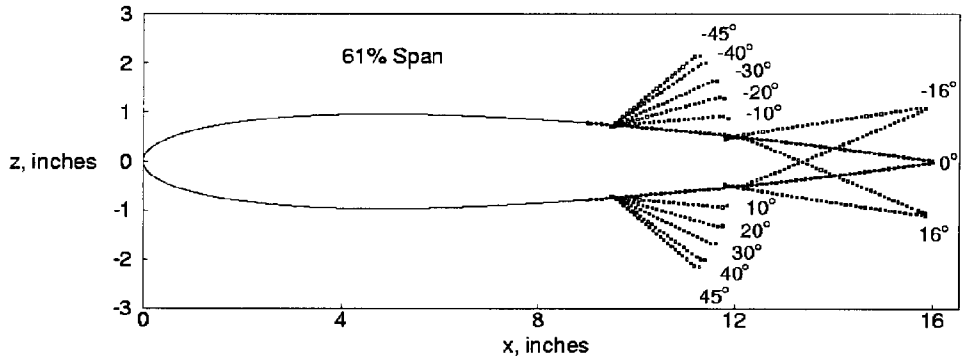

b) Ordinate measurements at 60% span.

Figure 5. Ordinate measurements for the BACT model.

Test Case	Point No	Wind-Off Zero Pt	TDT Test 485
8EST33	203	132	BmpBACT/Static

Mach No	q, psf	Rn*10**-6	gamma
0.769	145.4	3.83	1.132

alphao	delta te	delta us	delta ls	(degees)
3.99	5.00	0.10	-0.10	

C-Normal F	C-Pitch M	C-Axial F	C-Roll M	C-Yaw M
0.3675	0.1022	0.0108	0.2751	0.0216

Upper surface at ETA = 0.60

x/c	Cp Mean	Cp Min	Cp Max	CpStdDev	Chl No
0.000	1.106	1.078	1.135	0.018	82
0.010	-0.336	-0.386	-0.283	0.017	83
0.030	-0.686	-0.728	-0.641	0.017	84
0.060	-0.636	-0.687	-0.583	0.017	85
0.100	-1.119	-1.139	-1.098	0.017	86
0.150	-1.218	-1.246	-1.188	0.018	87
0.200	-1.315	-1.353	-1.270	0.021	88
0.250	-1.340	-1.377	-1.297	0.022	89
0.300	-1.065	-1.336	-0.583	0.170	90
0.350	-0.545	-0.746	-0.422	0.043	91
0.400	-0.399	-0.495	-0.322	0.024	92
0.450	-0.336	-0.453	-0.219	0.033	93
0.500	-0.296	-0.393	-0.200	0.027	94
0.530	-0.270	-0.367	-0.159	0.027	95
0.550	-0.298	-0.382	-0.189	0.027	96
0.570	-0.278	-0.359	-0.186	0.025	97
0.590	-0.230	-0.297	-0.168	0.017	98
0.610	-0.279	-0.399	-0.153	0.032	129
0.630	-0.252	-0.349	-0.157	0.028	130
0.660	-0.226	-0.314	-0.104	0.027	131
0.690	-0.227	-0.307	-0.127	0.026	132
0.720	-0.235	-0.312	-0.137	0.024	133
0.760	-0.296	-0.397	-0.172	0.030	134
0.790	-0.157	-0.234	-0.058	0.024	135
0.820	-0.073	-0.142	0.010	0.021	136
0.850	-0.015	-0.077	0.063	0.019	137
0.880	0.045	-0.012	0.104	0.017	138
0.910	0.110	0.059	0.158	0.014	139
0.950	0.162	0.112	0.213	0.014	140
1.000	0.213	0.169	0.259	0.013	141

Lower surface at ETA = 0.60

x/c	Cp Mean	Cp Min	Cp Max	CpStdDev	Chl No
0.010	0.720	0.674	0.771	0.017	114
0.030	0.284	0.228	0.342	0.016	113
0.060	0.065	0.015	0.118	0.014	112
		.			
		.			
0.910	0.110	0.066	0.150	0.012	143
0.950	0.155	0.132	0.177	0.007	142

Upper surface at ETA = 0.40

x/c	Cp Mean	Cp Min	Cp Max	CpStdDev	Chl No
0.600	-0.198	-0.304	-0.099	0.027	65
0.650	-0.160	-0.244	-0.072	0.026	66
		.			
		.			
0.950	0.124	0.081	0.185	0.015	72
1.000	0.212	0.181	0.254	0.010	73

Lower surface at ETA = 0.40

x/c	Cp Mean	Cp Min	Cp Max	CpStdDev	Chl No
0.600	-0.126	-0.202	-0.025	0.023	81
0.650	-0.083	-0.142	-0.007	0.019	80
		.			
		.			
0.900	0.085	0.035	0.146	0.014	75
0.950	0.127	0.081	0.181	0.014	74

Figure 6. Example of static control surface deflection data file for BACT.

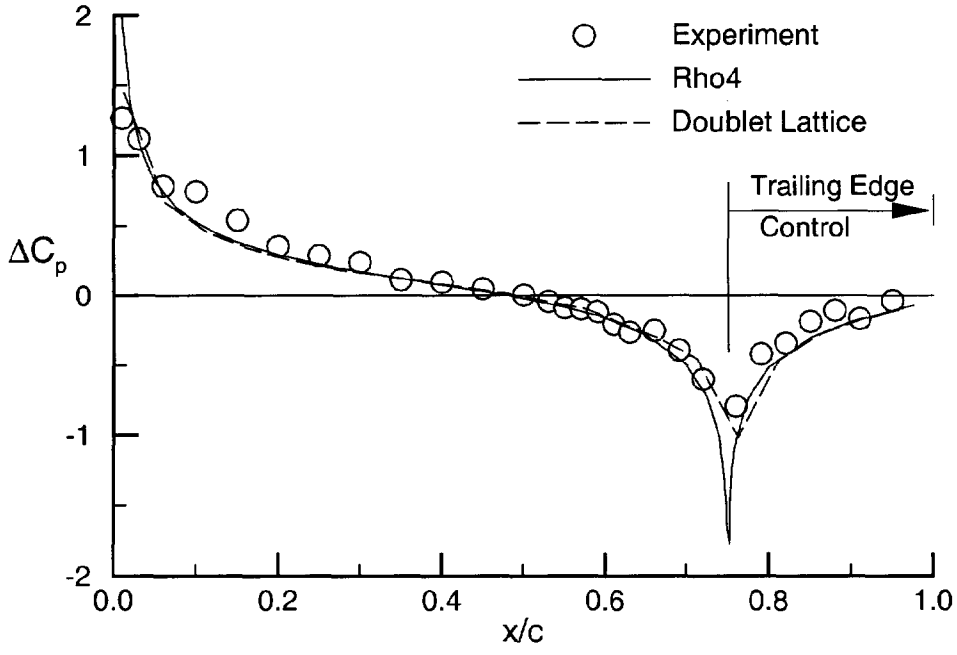

a) M=0.65, Test 485, Point 1945.

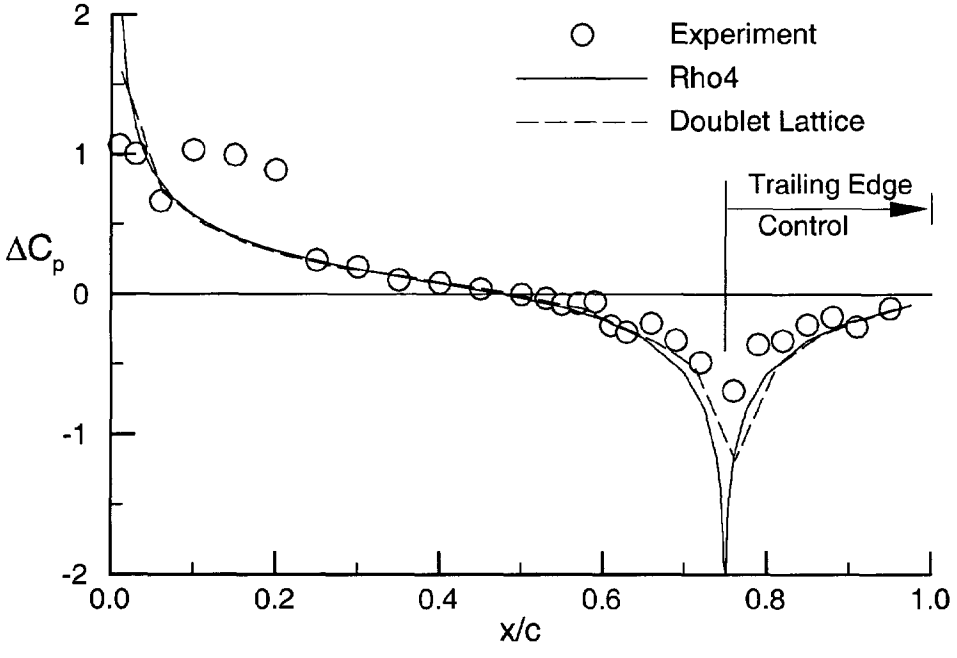

b) M=0.75, Test 485, Point 1686.

Figure 7. Comparison of BACT static results with linear aerodynamics, α=4° and δ_{TE}=-10°.

Test Case	Point No	Wind-Off Zero Pt	TDT Test 485
8EOT31	1094	1060	BmpBACT/TE Oscillations

Mach No	q, psf	Rn*10**-6	gamma	Vel, fps	freq, Hz	k
0.771	149.00	3.86	1.132	387.7	10.020	0.1083

alphao	delta teo	delta uso	delta lso	te osc ampl	(degees)
4.01	0.10	-0.12	0.14	3.87	

C-Normal-F	C-Pitch-M	C-Axial-F	C-Roll-M	C-Yaw-M (means)	nsamples
0.3013	0.0987	0.0079	0.2227	0.0161	4989

Upper surface at ETA = 0.60

x/c	Cp Mean	Cp Min	Cp Max	CpStdDev	Real(Cp)	Imag(Cp)	Chl No
0.000	1.093	1.065	1.131	0.008	-0.0021	0.0029	82
0.010	-0.328	-0.397	-0.267	0.019	-0.0068	0.0118	83
0.030	-0.705	-0.762	-0.645	0.016	-0.0053	0.0112	84
0.060	-0.638	-0.718	-0.578	0.018	-0.0068	0.0119	85
0.100	-1.096	-1.111	-1.076	0.005	-0.0007	0.0017	86
0.150	-1.228	-1.248	-1.203	0.006	-0.0017	0.0035	87
0.200	-1.252	-1.295	-1.205	0.012	-0.0041	0.0079	88
0.250	-1.288	-1.335	-1.224	0.014	-0.0049	0.0085	89
0.300	-0.926	-1.344	-0.514	0.203	-0.1579	0.0967	90
0.350	-0.493	-0.733	-0.358	0.051	-0.0383	0.0175	91
0.400	-0.401	-0.524	-0.318	0.029	-0.0211	0.0027	92
0.450	-0.334	-0.473	-0.213	0.037	-0.0205	-0.0032	93
0.500	-0.289	-0.418	-0.184	0.031	-0.0236	-0.0034	94
0.530	-0.270	-0.384	-0.153	0.032	-0.0261	-0.0036	95
0.550	-0.233	-0.342	-0.125	0.032	-0.0285	-0.0035	96
0.570	-0.223	-0.328	-0.122	0.032	-0.0306	-0.0034	97
0.590	-0.215	-0.301	-0.139	0.026	-0.0283	-0.0025	98
0.610	-0.227	-0.401	-0.072	0.056	-0.0657	-0.0055	129
0.630	-0.190	-0.355	-0.041	0.055	-0.0670	-0.0055	130
0.660	-0.167	-0.327	0.004	0.058	-0.0726	-0.0069	131
0.690	-0.150	-0.311	0.029	0.065	-0.0857	-0.0083	132
0.720	-0.100	-0.268	0.088	0.078	-0.1061	-0.0107	133
0.760	-0.087	-0.356	0.157	0.128	-0.1762	-0.0195	134
0.790	-0.057	-0.224	0.114	0.074	-0.0982	-0.0168	135
0.820	0.008	-0.106	0.134	0.049	-0.0612	-0.0146	136
0.850	0.052	-0.043	0.146	0.033	-0.0365	-0.0129	137
0.880	0.055	-0.019	0.135	0.023	-0.0193	-0.0107	138
0.910	0.155	0.100	0.218	0.016	-0.0098	-0.0087	139
0.950	0.197	0.148	0.251	0.015	-0.0005	-0.0059	140
1.000	0.266	0.209	0.316	0.015	-0.0052	-0.0017	141

Lower surface at ETA = 0.60

x/c	Cp Mean	Cp Min	Cp Max	CpStdDev	Real(Cp)	Imag(Cp)	Chl No
0.010	0.716	0.665	0.780	0.014	0.0057	-0.0071	114
0.030	0.272	0.211	0.340	0.017	0.0073	-0.0080	113
0.060	0.010	-0.046	0.069	0.016	0.0078	-0.0078	112
			.				
			.				
0.910	0.064	0.016	0.118	0.015	0.0080	0.0087	143
0.950	0.191	0.166	0.216	0.008	-0.0014	0.0059	142

Upper surface at ETA = 0.40

x/c	Cp Mean	Cp Min	Cp Max	CpStdDev	Real(Cp)	Imag(Cp)	Chl No
0.600	-0.201	-0.312	-0.082	0.033	-0.0270	-0.0050	65
0.650	-0.162	-0.269	-0.054	0.033	-0.0307	-0.0052	66
			.				
			.				
0.950	0.166	0.123	0.217	0.014	-0.0041	-0.0011	72
1.000	0.307	0.278	0.338	0.009	-0.0002	-0.0007	73

Lower surface at ETA = 0.40

x/c	Cp Mean	Cp Min	Cp Max	CpStdDev	Real(Cp)	Imag(Cp)	Chl No
0.600	-0.144	-0.249	-0.032	0.033	0.0310	-0.0018	81
0.650	-0.111	-0.206	-0.012	0.033	0.0356	-0.0007	80
0.700	-0.077	-0.168	0.038	0.035	0.0398	0.0011	79
			.				
			.				
0.900	0.094	0.030	0.154	0.019	0.0154	0.0019	75
0.950	0.160	0.105	0.216	0.016	0.0078	0.0008	74

Figure 8. Example of oscillating control surface data file for BACT.

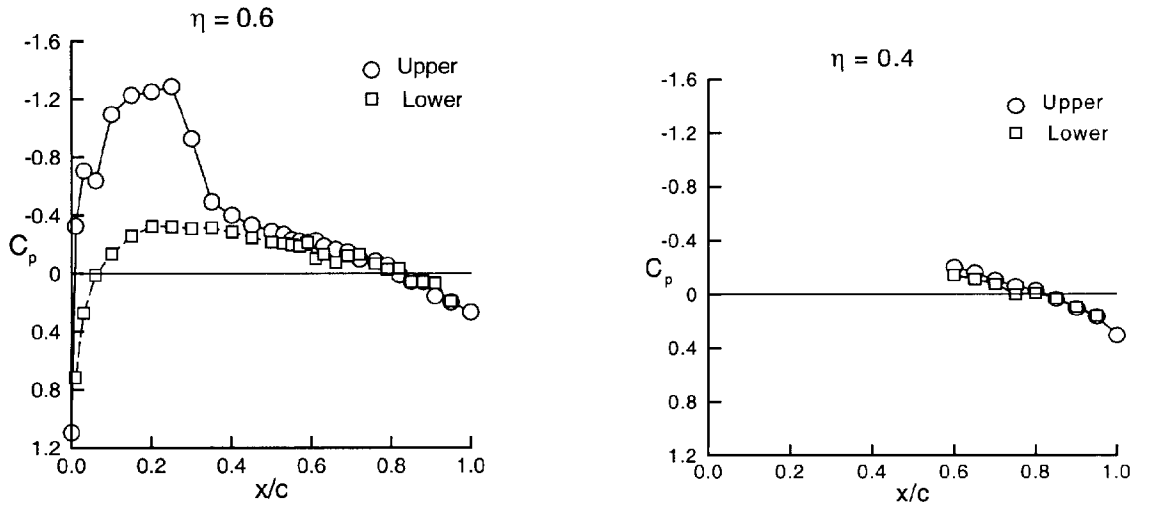

(a) Mean pressure coefficient during control surface oscillation

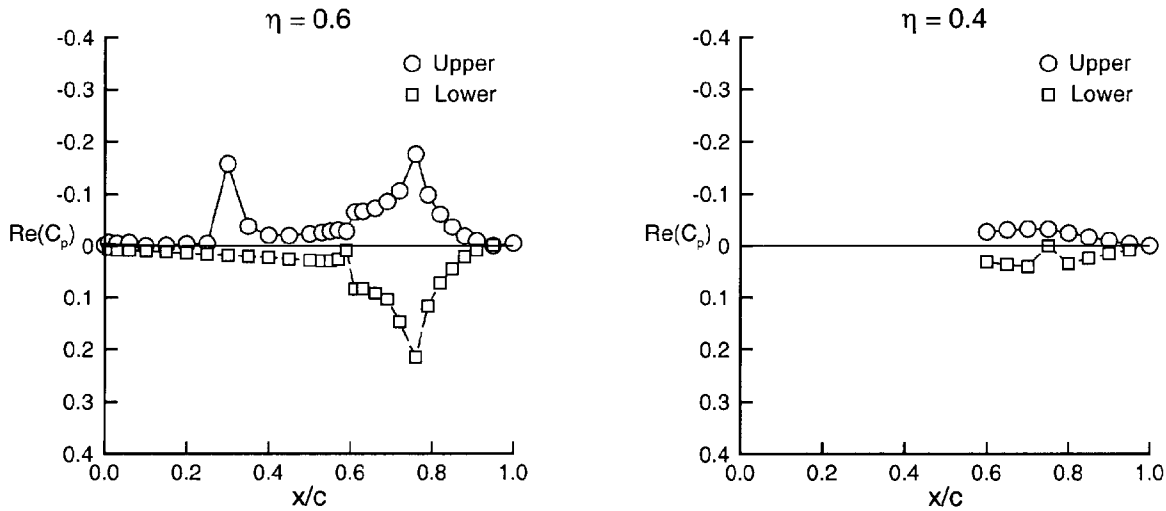

(b) Real part of pressure coefficient during control surface oscillation

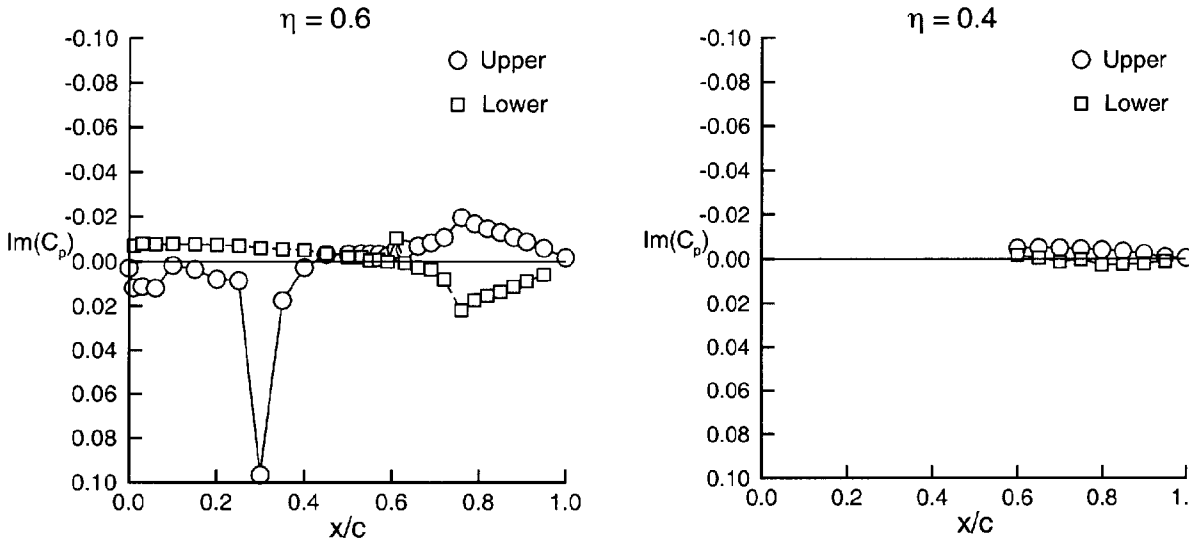

(c) Imaginary part of pressure coefficient during control surface oscillation

Figure 9. Unsteady pressures measured during trailing edge control oscillations, Test Case 8EOT31, M=0.77, $\alpha = 4^{o}$.

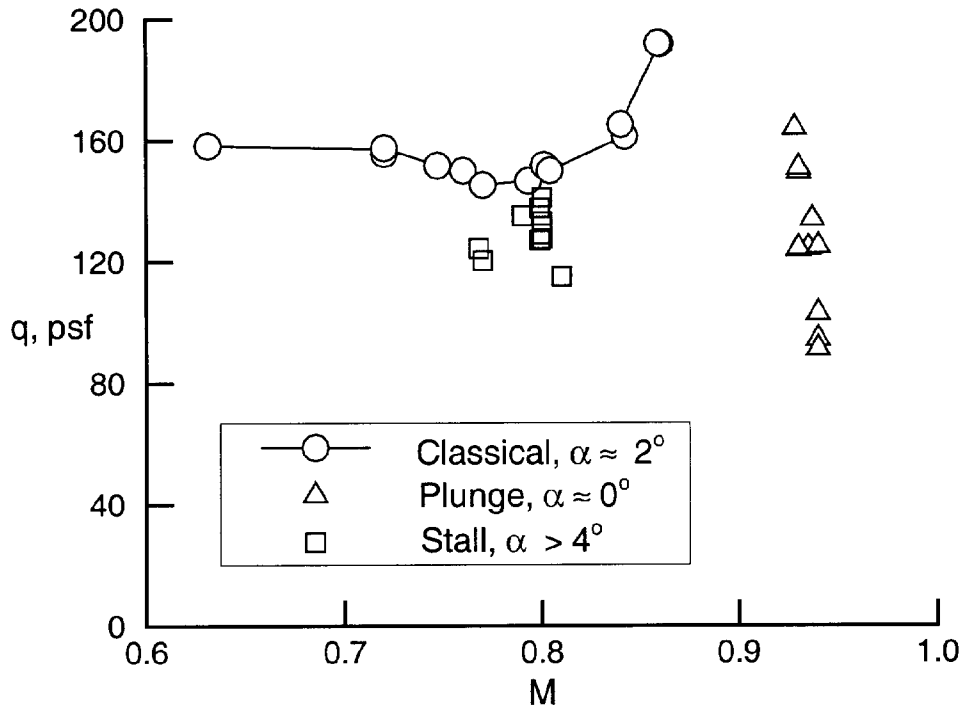

(a) Flutter dynamic pressure.

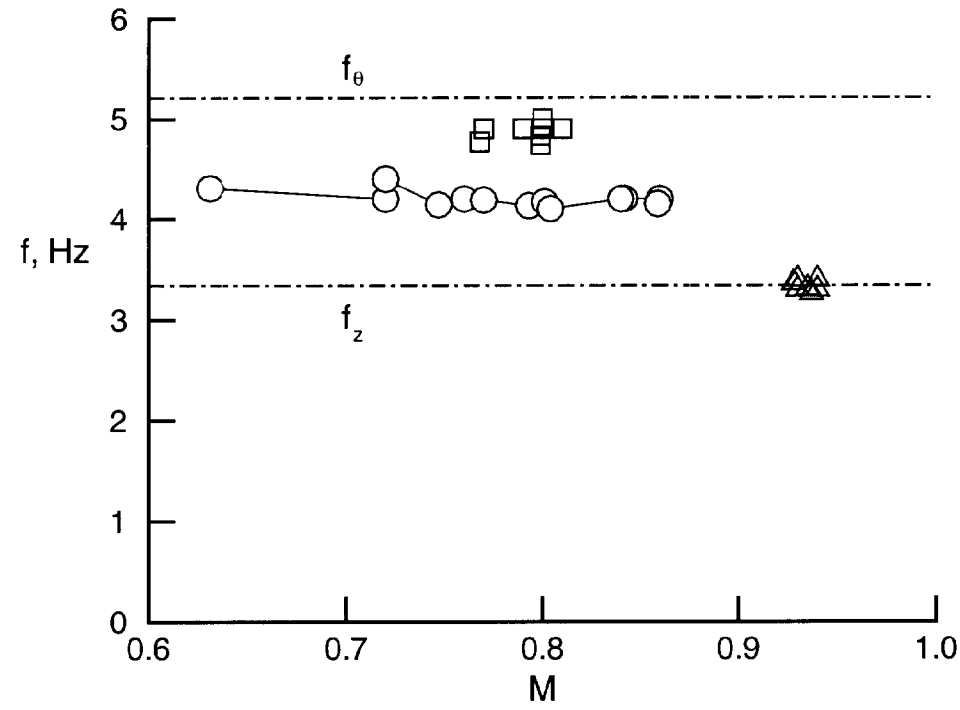

(a) Flutter frequencies.

Figure 10. BACT flutter instabilities.